JMEPEG (2022) 31:4955–4962
https://doi.org/10.1007/s11665-022-06596-9

1059-9495/$19.00

TECHNICAL ARTICLE

Tribological Properties and Electrical Conductivity of Carbon Nanotube-Reinforced Copper Matrix Composites

Shaoli Fu, Xiaohong Chen, Ping Liu, Haipo Cui, Honglei Zhou, Fengcang Ma, and Wei Li

Submitted: 5 August 2021 / Revised: 20 October 2021 / Accepted: 5 January 2022 / Published online: 3 March 2022

Carbon nanotube-reinforced copper matrix (CNT/Cu) composites were prepared by a method involving solution-aging treatment, in situ chemical vapor deposition (CVD), and spark plasma sintering (SPS). The tribological properties of the CNT/Cu composites were greatly improved, and the friction stability was better than that of Cu. These performance improvements were attributed to the uniform distribution of the CNTs without agglomeration and the strong interfacial bonding between the Cu matrix and CNTs. The coefficient of friction was 0.2, which was lower than that of pure copper (0.55), and the wear rate of the CNT/Cu composites was 2 times lower than that of pure copper. The wear mechanism was also discussed from the perspective of the wear morphology and interface structure. Furthermore, the electrical conductivity remained at a high level. The preparation technique is simple and easy to be controlled and can be used to synthesize CNT/Cu composites with excellent tribological properties and electrical conductivity.

Keywords carbon nanotubes, chemical vapor deposition, copper matrix composites, solution-aging treatment, spark plasma sintering, tribological properties

1. Introduction

Copper-based composites play a crucial role in railway, military vehicles, electrical components, electrical contact materials, special conductors and other fields due to their outstanding electrical and thermal conductivity and good wear resistance (Ref 1-7). However, with the rapid development of the railway and automobile industries, there is a high demand for new materials with improved tribological properties that maintain their good electrical conductivity. Examples of such materials include pantograph sliders for high-speed trains, electric brushes, and other sliding electrical contact materials. CNTs are an ideal enhancement phase for improving the properties of copper alloys due to their excellent comprehensive properties, such as low density, high strength, and high Young's modulus (Ref 8-11). CNT-reinforced metal matrix composites are self-lubricating materials due to their outstanding friction properties (Ref 12). Thus, they can improve the wear resistance and reduce the coefficient of friction, while also eliminating the need for external lubricants to avoid jamming, which makes them potential structural materials in the aerospace and automotive fields (Ref 13-15). The tribological properties of CNT/Cu composites have been investigated in recent years (Ref 16-19). For example, Dong et al. (Ref 20) prepared a Cu-matrix composite reinforced by CNTs using powder metallurgy, which displayed a lower coefficient of friction and reduced weight loss. Kim et al. (Ref 21) prepared Cu/CNT composites by a molecular-level technique and SPS, and showed that the friction properties of the composites were three times higher than that of pure copper. Xu et al. (Ref 22) mixed copper powders and CNTs by ball milling and prepared CNT-Cu composites by powder metallurgy. The wear mechanism of the CNT-Cu composites was mainly adhesive wear and plastic flow deformation. However, due to the randomness of the ball milling process (Ref 23), it was difficult to obtain a homogeneous dispersion while maintaining the integrity of the CNTs, which greatly weakened the self-lubrication property of the CNTs. In addition, some impurities may be introduced during ball milling. Guiderdoni et al. (Ref 24) prepared CNT/Cu composites by SPS, which had a hardness that was 1.5 times that of pure copper, and a coefficient of friction and wear rate that were, respectively, 3-4 times and 10-20 times lower than that of pure copper. Huang et al. (Ref 25) prepared aligned CNT-reinforced copper-based composites by electroless plating, ultrasonic mechanical stirring, sintering, forging and die drawing. The coefficient of friction and wear rate were decreased by 68 and 90.2% compared with pure copper, respectively.

Although the composites prepared by the above processes showed improved friction properties, the CNTs required acidification, cleaning, drying, and other relatively complicated processes that made it difficult to ensure a repeatable preparation process. In addition, surface modification can damage CNTs, causing them easy to agglomerate due to strong van der Waals force among them. Therefore, it is difficult to ensure good dispersion of CNTs in the copper matrix and strong interfacial bonding between Cu matrix and CNTs, which prevents the full utilization of the excellent properties of CNTs (Ref 26). Hence, there is a need for a method to prepare CNTs

Shaoli Fu, Xiaohong Chen, Ping Liu, Honglei Zhou, Fengcang Ma, and **Wei Li**, School of Materials and Chemistry, University of Shanghai for Science and Technology, Shanghai 200093, China; **Haipo Cui**, School of Health Science and Engineering, University of Shanghai for Science and Technology, Shanghai 200093, China. Contact e-mail: cxhusst@163.com.

with complete structure, and ensure that they are uniformly dispersed in the Cu matrix. Moreover, the preparation technology should be simple, repeatable and easy to operate.

The in situ chemical vapor deposition (CVD) method can ensure the good growth of CNTs, and SPS has the advantages of fast heating rate, short sintering time and low sintering temperature (Ref 27-29), which greatly improve the production efficiency and save much energy. Therefore, CNT/Cu composites were prepared by a new process that involved solution-aging treatment, in situ CVD and SPS.

2. Experimental

CuCr (0.6 wt.% Cr, ≤ 200 mesh, Changsha Tianjiu metal material Co., Ltd, China) alloy powders were annealed at 550 °C for 30 min to remove residual oxides on the surface. Then, the CuCr alloy powders were solution-treated at 850 °C for 1 h and aging treated at 450 °C for 2 h under a mixed atmosphere with a flow rate of 1650 mL/min (Ar) and 1350 mL/min (H_2) to uniformly disperse the Cr particles in the copper matrix. Cr was used to catalyze the growth of CNTs without reducing the electrical conductivity of the copper matrix due to its low solid solubility in Cu. Then, CNT/Cu composite powders were synthesized by in situ CVD at 800 °C for 60 min, with a C_2H_4 : Ar+H_2O : H_2 gas ratio of 100: 1200: 2450 (mL/min). All the gases were provided by Shanghai Jiangnan Gas Co., Ltd. The heat treatment was performed in a tubular furnace with a diameter of 80 mm (OTF-1200X, Hefei Kejing material technology Co., Ltd, China). The size of the CNT/Cu composite samples was ∅30 mm × 3 mm (height). Five samples were studied for each test, and the average was reported. Finally, we prepared CNT/Cu composites by SPS (750 °C, 10 min, 45 MPa). The CNTs were uniformly distributed in the Cu matrix without agglomeration, and the graphite lattice diffused to the Cu lattice at the interface, so the interfacial bonding between Cu and CNTs was strong. Thus, the tribological properties of the CNT/Cu composites significantly improved compared with Cu under keeping the electrical conductivity at a high level. In addition, the volume fraction of CNTs in the CNT/Cu composites is 0.5%. Cu samples were used for comparison. The preparation process flow is shown in Fig. 1.

The morphologies of the CNT/Cu composites were observed by scanning electron microscope (SEM, Quanta FEG 450 FEI USA). Transmission electron microscope (TEM, Tecnai G2 F30 FEI USA) was utilized to characterize the CNT/Cu composite interfaces. The friction-wear properties were analyzed using a reciprocating friction-wear tester (HSR-2M, Lanzhou Zhongke Kaihua Technology development Co., Ltd China). Three-dimensional optical microscope (Contour GT-K Bruker USA) was used to investigate the morphologies and three-dimensional roughness of the wear scars. A digital metal conductivity tester (D60K, Xiamen Xinbot Technology Co., Ltd, China) was used to measure the electrical conductivity of Cu and CNT/Cu composites.

3. Results

3.1 Characterization of CNT/Cu Composite Powders

Figure 2(a) shows the SEM images of the CuCr alloy powders. The uniform distribution of Cr particles in the copper matrix provided a foundation for the homogenous growth of CNTs. Figure 2(b), (c) and (d) illustrates the CNTs prepared by *in situ* CVD. The CNTs grew uniformly (Fig. 2b) and independently of each other without agglomeration (Fig. 2c). By reducing the CVD reaction time, the number of CNTs was reduced and their length was shortened. The blue circle in Fig. 2(d) shows that one end of the CNTs was completely embedded in the copper matrix. This can limit the CNT's movement and reduce their agglomeration, thereby ensuring their homogeneous dispersion and improving the wettability between Cu and CNTs. The TEM images of the CNTs in Fig. 2(e) and the inset (e_1) show that the CNTs are hollow multi-walled tubes with uniform diameters of about 20.16 nm. Furthermore, the walls are smooth and clean with few defects. Figure 2(f) shows the Raman spectrum of the CNT/Cu composite powders. The I_D/I_G is about 0.909, which indicates that the degree of graphitization of CNTs was good, and the defect density was small. Thus, it can be concluded that high-quality CNT/Cu composite powders were prepared by this process, which laid the foundation for the preparation of CNT/Cu composites with good friction performance and electrical conductivity.

3.2 Electrical Conductivity and Friction Properties of CNT/Cu Composites

The CNTs with complete structure are important to the properties of CNT/Cu composite. Therefore, the SEM on the CNT structural intactness in the final bulk CNT/Cu composites are displayed in Fig. 3(a). It is shown in Fig. 3(a) that the CNTs in the bulk CNT/Cu composite had a complete structure without fracture or breakage. Figure 3(b) compares the friction coefficients of Cu and CNT/Cu composites and the loading time. Both friction coefficients greatly fluctuated during the initial stage of the test because of the polishing process during the wear test period, i.e., the surface of the wear track was smoothed by grinding away the uneven surface (Ref 30). We also found that the friction stability of the CNT/Cu composites was better than that of Cu, which is one of the important characteristics of friction materials (Ref 31, 32). After 30 s, the coefficient of friction of both the Cu and CNT/Cu composites is stabilized at 0.55 and 0.2, respectively. Due to the good self-lubricity of the CNTs (Ref 20), they can form a protective film on the surface of CNT/Cu composites. During friction and wear processes, the CNTs gradually bent and deformed until they were destroyed at longer friction times. The fragments formed by the broken CNTs accumulated and diffused between the wear surface and grinding ball to form a self-lubricating film that slowed damage to the CNT/Cu composites. The interfacial bonding between the CNTs and Cu matrix was very good, giving the CNT/Cu composites high densification, which prevented the interfacial scattering from affecting the electrical conductivity. Therefore, the CNT/Cu composites displayed an excellent electrical conductivity of 92.9% IACS, and the relative density and electrical conductivity as shown in Fig. 3(c). The Vickers hardness of the CNT/Cu composites (102 HV) was higher than that of Cu (82 HV) (Fig. 3c) (Ref 33). All of the above factors show that the friction properties of the CNT/Cu composites were better than pure copper, which can reduce the damage to CNT/Cu composites.

Figure 4(a) and (b) shows the SEM images of the friction-wear morphologies of Cu and CNT/Cu composites. It can be seen that the wear width of Cu and CNT/Cu composites was

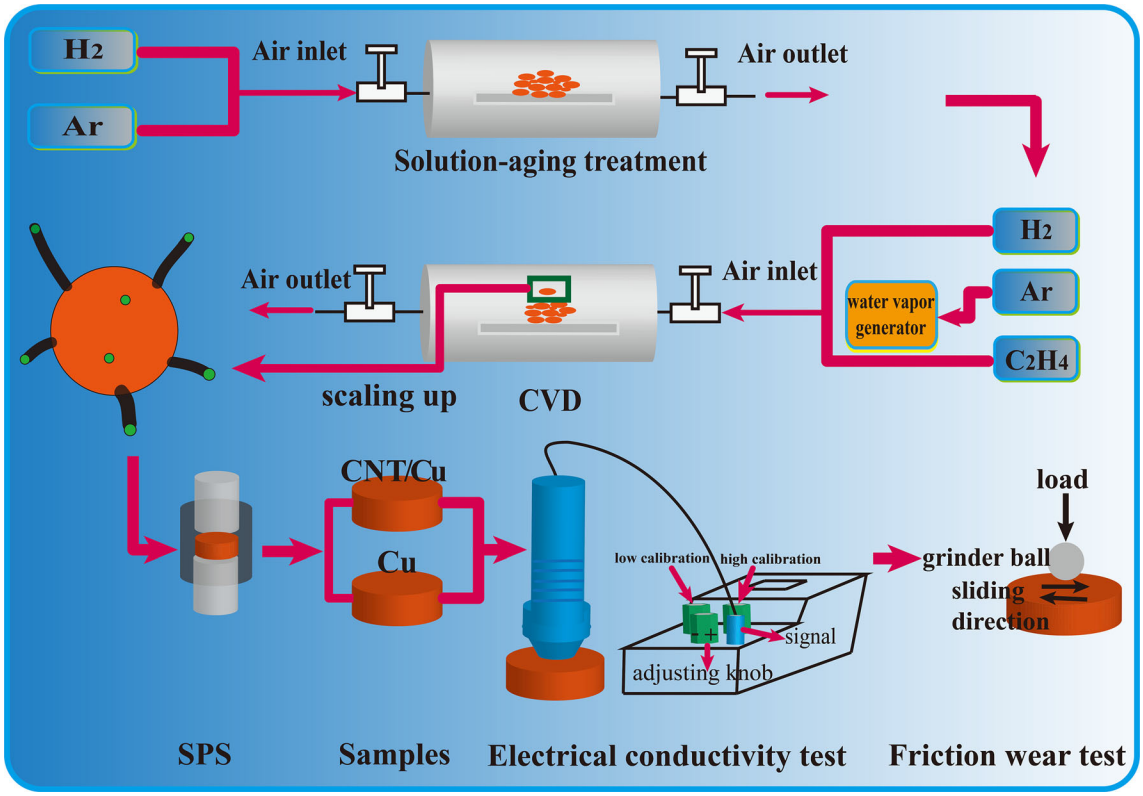

Fig. 1 Schematic diagram of the preparation process of CNT/Cu composites

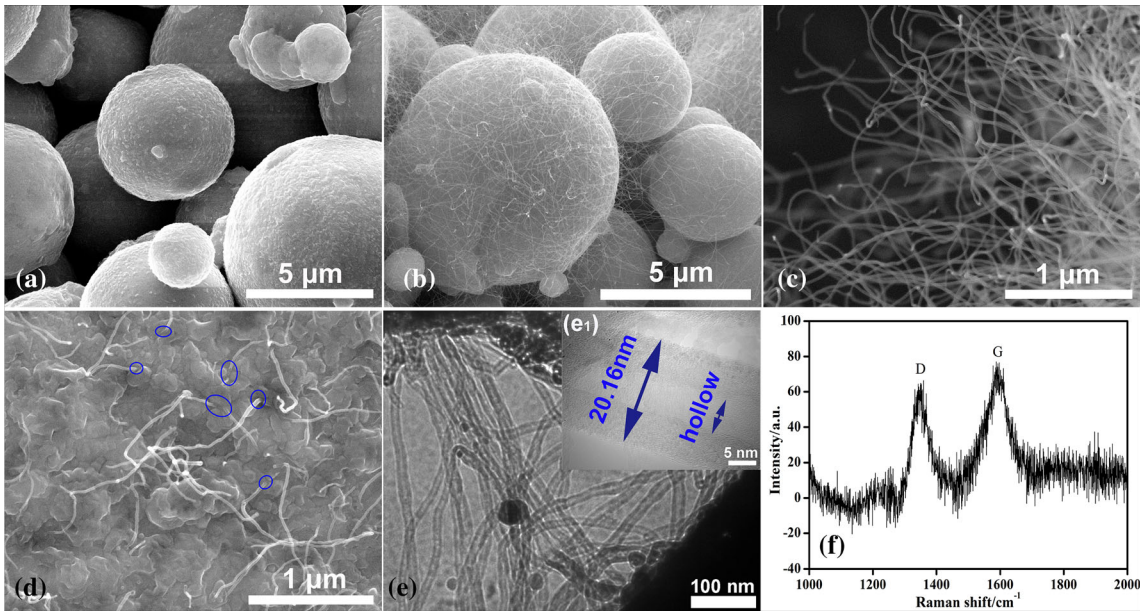

Fig. 2 SEM images of (a) CuCr alloy powders, (b, c, d) CNT/Cu composite powders, (e, e1) TEM images, and (f) Raman spectrum of CNT/Cu composite powders

825 and 520 μm, respectively, and there were many exfoliated fragments and grooves on the friction-wear surface of Cu (Ref 34). This showed that the main wear mechanism of Cu was serious adhesive wear (Ref 35, 36) because the contact stress caused plastic flow on the contact surface, accompanied by a large amount of heat, which melted the contact interface and underwent micro-welding. These factors made the wear areas form peeling marks that eventually formed grooves and debris (Ref 37, 38). The self-protection of the CNT/Cu composites was enhanced because the uniformly-distributed CNTs provided good self-lubricity and superior load transfer between the Cu matrix and CNTs (Ref 39, 40). Hence, only an extremely weak lamellar phenomenon was observed at the edges, as shown in Fig. 4(b).

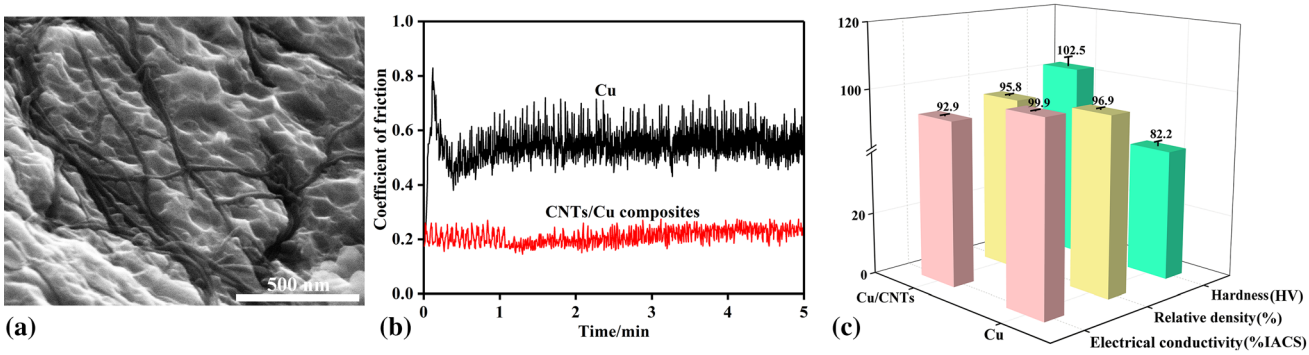

Fig. 3 (a) SEM image of the CNTs in the final bulk CNT/Cu composites, Properties of Cu and CNT/Cu composites (b) coefficient of friction (c) electrical conductivity, relative density and Vickers hardness

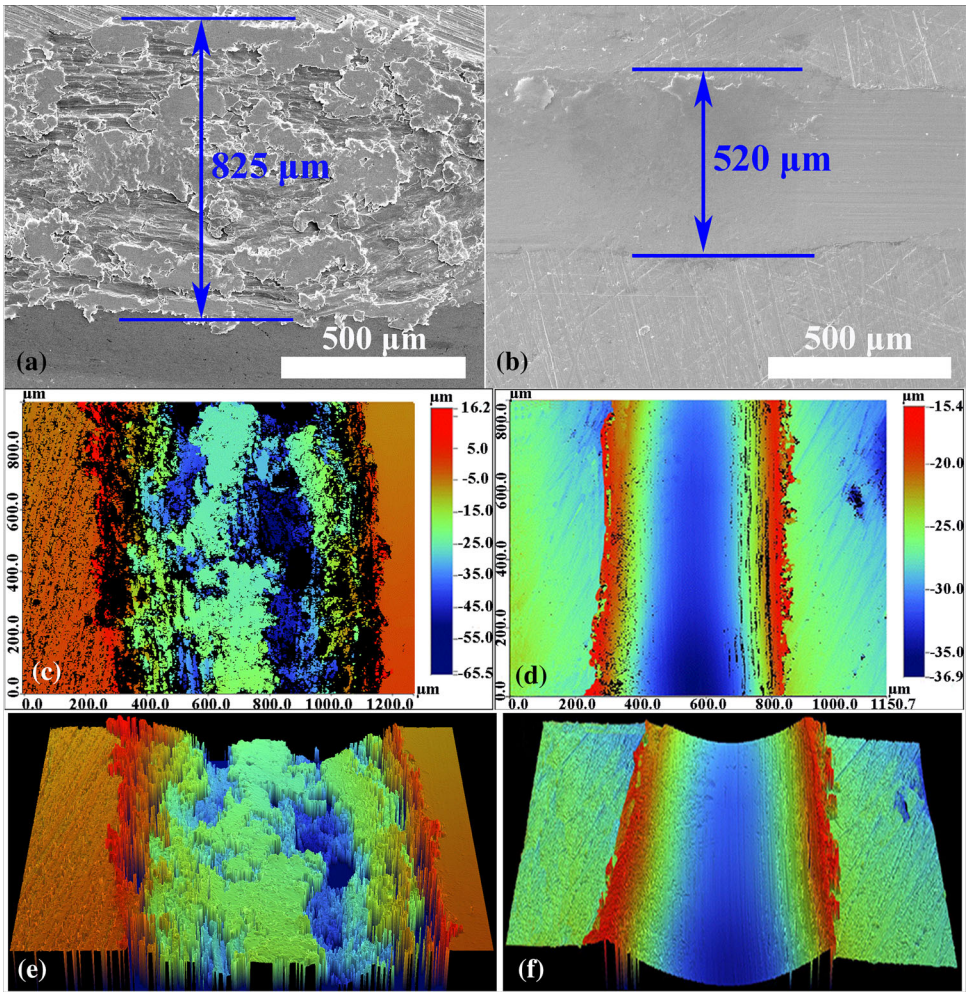

Fig. 4 SEM images of the friction-wear morphologies of Cu (a) and CNT/Cu composites (b), three-dimensional morphologies of the wear scars of Cu (c, e) and CNT/Cu composites (d, f)

Figure 4(c, e) and (d, f) shows the depth, width, and roughness of the three-dimensional morphologies of the wear scars of Cu and CNT/Cu composites. The wear surface of pure Cu was relatively rough and contained grooves, while the wear surface of the CNT/Cu composites was smoother, as shown in Fig. 4(d, f). The results were in agreement with SEM observations.

Figure 5 shows the 3D roughness characterization parameters (S_{ku}, S_{sk}, S_a, S_q, S_z) of the surface pure Cu and CNT/Cu composites. The kurtosis of the surface height distribution S_{ku} were 1.778 and 1.121 for Cu and CNT/Cu composites, indicating a scattered distribution ($S_{ku} < 3$). The skewness S_{sk} (-1.268 and -1.045) of both materials was less than 0, indicating that the height distribution was higher than that of the average plane. The arithmetic average deviation S_a, the root

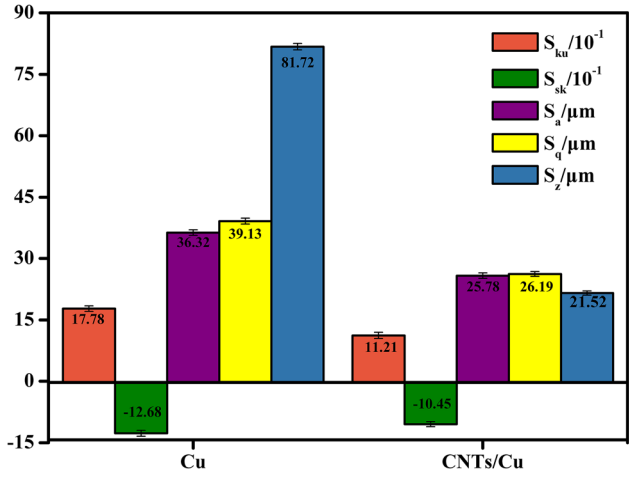

Fig. 5 3D roughness characterization parameters (S_{ku}, S_{sk}, S_a, S_q, S_z) of the wear surface of pure copper and CNT/Cu composites

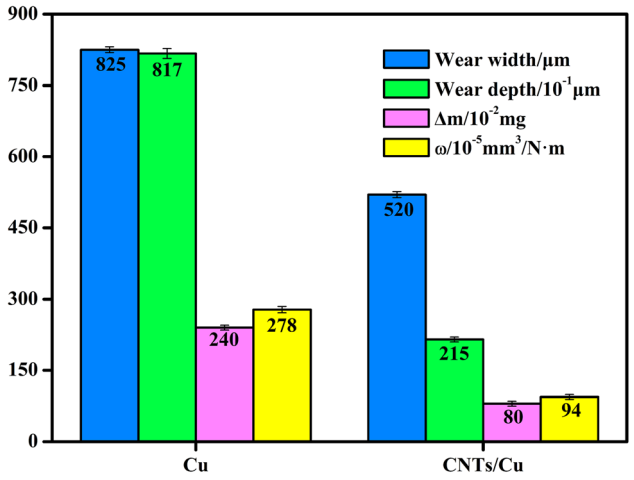

Fig. 6 Wear width, wear depth, wear mass and wear rate for Cu and CNT/Cu composites

mean square deviation S_q, and the ten-point height S_z of the CNT/Cu composites were smaller than those of pure Cu, demonstrating that the wear surface of the CNT/Cu composites was smoother. Therefore, the wear resistance of the CNT/Cu composites was much better than pure copper.

Wear rate is an important parameter for friction materials, so it is necessary to calculate the wear rate of Cu and CNT/Cu composite. The number of wear test repeats was five. The wear rate can be calculated by the following formula (Ref 41, 42):

$$\omega = \frac{\Delta V}{F \cdot d} = \frac{\Delta m}{\rho \cdot F \cdot d} \quad \text{(Eq 1)}$$

Where ω is the wear rate, ΔV is the worn volume, F is the applied load (10 N), d is the sliding distance (10 m), Δm is the worn mass and ρ is the density of the materials (ρ_{Cu}=8.63g/cm^3, $\rho_{CNT/Cu}$=8.51g/cm^3). Figure 6 shows that the wear width and wear depth is less than copper, and the wear rate of the CNT/Cu composites was about 2 times lower than that of Cu. Hence, the tribological properties of CNT/Cu are significantly improved owing to the present of CNTs.

4. Discussion

4.1 Wear Mechanism

It is crucial to investigate the chemical composition and bonding state of the wear surface to study the wear mechanism. Therefore, XPS analysis was performed on the wear surfaces of Cu and CNT/Cu composites. Figure 7(a) shows the full XPS spectra of the wear surface of Cu and CNT/Cu composites. The wear surface of pure copper contained only Cu and O peaks, while Cr and C peaks appeared on the wear surface of CNT/Cu composites. The intensity of the C peak was relatively large, indicating a high carbon content. Figure 7(b) shows that the main C 1s peak appeared at 284.5 eV, which was ascribed to sp^2 hybridized carbon, and the minor peak at 285.7 eV was attributed to sp^3 hybridized carbon (Ref 43). The results showed that the CNT/Cu composites contained a high CNTs content, which formed a self-lubricating film on the wear surface during the friction-wear process, which slowed damage to the CNT/Cu composites surface caused by the friction pair. This is in agreement with the SEM and three-dimensional morphology of the wear surface shown in Fig. 4. In addition, since Cr acted as a catalyst for CNTs growth, it was present throughout the whole process, and a Cr peak appeared in the XPS spectrum of the CNT/Cu wear surface.

Figure 7(c) displays the wear mechanism of Cu and CNT/Cu composites. When the friction pair slides across the Cu surface, the shedding of abrasive debris accelerated the stripping of particles from the surface (Ref 21). In the CNT/Cu composites, the CNTs nailed the Cu particles due to strong interfacial bonding, making it difficult for the copper particles to be separated from the composites surface. Meanwhile, CNTs acted as a lubricant film during the friction and wear processes. All these served to reduce the coefficient of friction, so the tribological properties of the CNT/Cu composites were better than that of Cu.

4.2 Interface Characterization

The interface diagram of the CNT/Cu composites in Fig. 8 shows that the interface between CNTs and Cu matrix was well bonded and that the graphite lattice of the CNTs diffused into the Cu lattice (Ref 44). This indicates that CNTs directly nucleated in the Cu matrix during the in situ synthesis of CNT/Cu composite powders. Therefore, carbon and copper atoms can undergo mutual diffusion, and the composites displayed Cu-Cu, C-C, and Cu-C bonds at the interface. The inverse fast Fourier transform (IFFT) C_1 and the interplanar spacing C_2 for area C in Fig. 8 showed that the matrix was Cu. The Fourier transformation A_1 and inverse fast Fourier transform A_2 of area A showed the presence of Cu and Cu_2O from the calculation interplanar spacing of 0.207 nm (Fig. A3) and 0.302 nm (Fig. A4). The diffraction spot calibration in Fig. B1 and the interplanar spacing 0.302 nm calculated from B_2 and B_3 verified the presence of the Cu_2O (110) crystal plane, which can improve the wettability between Cu and CNTs, leading to strong interfacial bonding. Thus, the CNT/Cu matrix interface remained flat and straight, with no accumulated dislocations and no obvious lattice distortion. Therefore, the interfacial scattering resistance, which is the main factor affecting the electrical conductivity, did not significantly change after the introduction of CNTs. Additionally, the CNTs have excellent electrical conductivity. We can see that the atoms of the CNTs

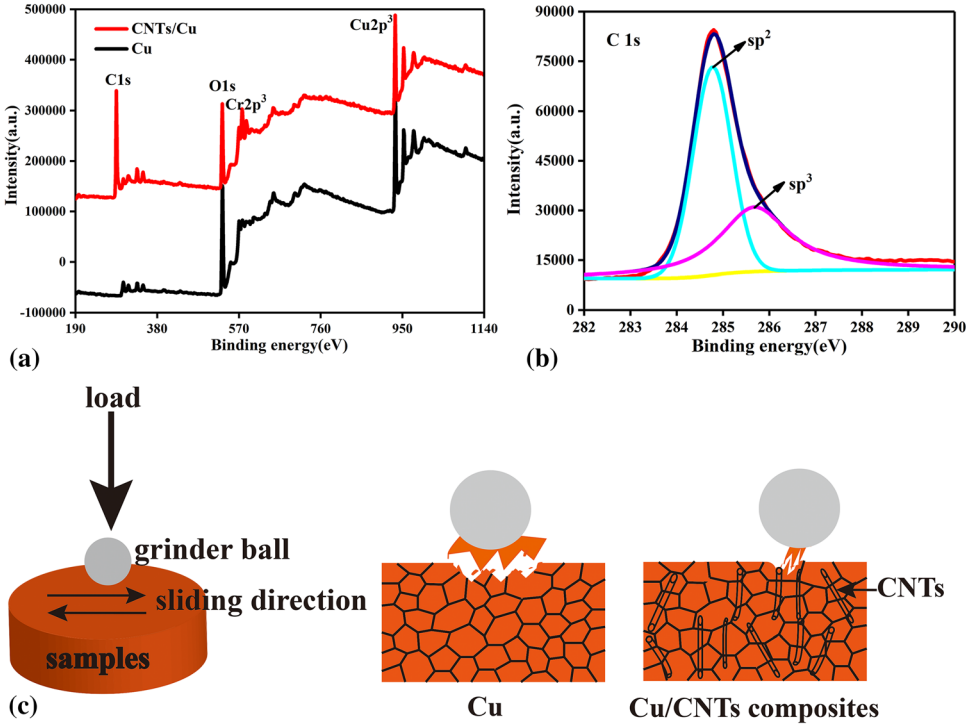

Fig. 7 (a) XPS full spectra, (b) curve-fitted XPS spectra of C 1s, (c) schematic illustration of the wear mechanism of Cu and CNT/Cu composites

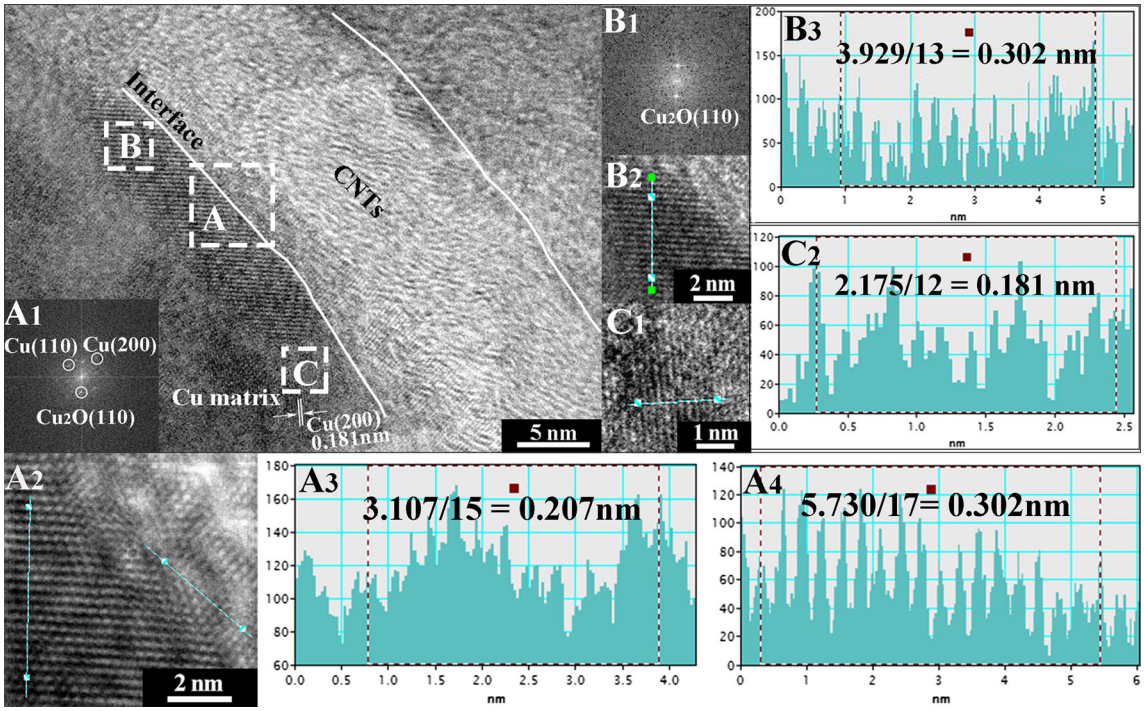

Fig. 8 The interfacial structure of CNT/Cu composites. A_1 (A_2) and B_1 (B_2) are FFT (IFFT) images of the region A and B. C1 is IFFT image for region C. A_3, A_4, B_3 and C_2 are the calculated interplanar spacings

in Fig. 8 were neatly arranged without an obvious bamboo-like structure or spiral or distortion caused by lattice misalignment. Although these CNTs are not completely metallic, they still improved the overall electrical conductivity of the composites. Therefore, the wear resistance of the CNT/Cu composites was improved and the electrical conductivity was maintained.

5. Conclusion

Cr particles were evenly distributed in the Cu matrix after CuCr alloy powders were treated by a solution-aging treatment to obtain a homogeneous CNTs dispersion without agglomeration in the Cu matrix. Meanwhile, strong interfacial bonding was observed between the CNTs and Cu in the CNT/Cu composites, which was responsible for the improved tribological properties and friction stability compared with Cu. Furthermore, the electrical conductivity of CNT/Cu remained high at 92.9% IACS. The precursor powders could be obtained by a solution-aging treatment, providing a process that is simple and easy to control. Thus, this study provides guidance for synthesizing CNT/Cu composites.

Acknowledgments

This work was supported by the National Key R&D Program of China (Grant No. 2017YFB0306405), the State Key Laboratory of Advanced Optical Communication Systems and Networks (Grant No. 2018GZKF03007), and the National Natural Science Foundation of China (Grant No. 51201107).

References

1. H. Kato, I.Y. TakamaM, K. Washida and Y. Sasaki, Wear and Mechanical Properties of Sintered Copper-tin Composites Containing Graphite or Molybdenum Disulfide, *Wear*, 2003, **255**, p 573–578. https://doi.org/10.1016/S0043-1648(03)00072-3
2. A.P. Zhilyaev, A. Morozova, J.M. Cabrera, R. Kaibyshev and T.G. Langdon, Wear Resistance and Electroconductivity in a Cu-0.3Cr-0.5Zr Alloy Processed by ECAP, *J. Mater. Sci.*, 2017, **52**(1), p 305–313. https://doi.org/10.1007/s10853-016-0331-8
3. D.B. Miracle, Metal Matrix Composites–From Science to Technological Significance, *Compos. Sci. Technol.*, 2005, **65**(15), p 2526–2540. https://doi.org/10.1016/j.compscitech.2005.05.027
4. A. Azarniya, A. Azarniya, S. Sovizi, H.R.M. Hosseini, T. Varol, A. Kawasaki and S. Ramakrishnad, Physicomechanical Properties of Spark Plasma Sintered Carbon Nanotube-Reinforced Metal Matrix Nanocomposites, *Prog. Mater. Sci.*, 2017, **90**, p 276–324. https://doi.org/10.1016/j.pmatsci.2017.07.007
5. Z.D. Shi, J. Sheng, Z.Y. Yang, Z.Y. Liu, S. Chen, M. Wang, L.D. Wang and W.D. Fei, Facile Synthesis of High-Performance Carbon Nanosheet/Cu Composites from Copper Formate, *Carbon*, 2020, **165**, p 349–357. https://doi.org/10.1016/j.carbon.2020.04.061
6. F. Daneshvar, S. Tagliaferri, H. Chen, T. Zhang, C. Liu and H.J. Sue, Ultralong Electrospun Copper−Carbon Nanotube Composite Fibers for Transparent Conductive Electrodes with High Operational Stability, *ACS Appl. Electron. Mater.*, 2020, **2**, p 2692–2698. https://doi.org/10.1021/acsaelm.0c00466
7. R. Shu, X.S. Jiang, H.L. Sun, Z.Y. Shao, T.F. Song and Z.P. Luo, Recent Researches of the Bio-Inspired Nano-Carbon Reinforced Metal Matrix Composites, *Compos. A Appl. Sci. Manuf.*, 2020, **131**, p 1–22. https://doi.org/10.1016/j.compositesa.2020.105816
8. S. Iijima, Helical Microtubules of Graphitic Carbon, *Nature*, 1991, **354**(6348), p 56–58. https://doi.org/10.1038/354056a0
9. S.S. Xie, W.Z. Li, Z.W. Pan, B.H. Chang and L.F. Sun, Mechanical and Physical Properties on Carbon Nanotube, *J. Phys. Chem. Solids*, 2000, **61**(7), p 1153–1158. https://doi.org/10.1016/S0022-3697(99)00376-5
10. C. Laurent, E. Flahaut and A. Peigney, The Weight and Density of Carbon Nanotubes versus the Number of Walls and Diameter, *Carbon*, 2010, **48**(10), p 2994–2996. https://doi.org/10.1016/j.carbon.2010.04.010
11. M.F. Yu, O. Lourie, M.J. Dyer, K. Moloni, T.F. Kelly and R.S. Ruoff, Strength and Breaking Mechanism of Multiwalled Carbon Nanotubes under Tensile Load, *Science*, 2000, **287**(5453), p 637–640. https://doi.org/10.1126/science.287.5453.637
12. F. Akhlaghi and A. Zare-Bidaki, Influence of Graphite Content on the Dry Sliding and Oil Impregnated Sliding Wear Behavior of Al 2024 – Graphite Composites Produced by in situ Powder Metallurgy Method, *Wear*, 2009, **266**(1), p 37–45. https://doi.org/10.1016/j.wear.2008.05.013
13. A.D. Moghadam, E. Omrani, P.L. Menezes and P.K. Rohatgi, Mechanical and Tribological Properties of Self-Lubricating Metal Matrix Nanocomposites Reinforced by Carbon Nanotubes (CNTs) and Graphene–A Review, *Compos. B Eng.*, 2015, **77**, p 402–420. https://doi.org/10.1016/j.compositesb.2015.03.014
14. A.D. Moghadam, B.F. Schultz, J.B. Ferguson, E. Omrani, P.K. Rohatgi and N. Gupta, Functional Metal Matrix Composites: Self-lubricating, Self-healing, and Nanocomposites-An Outlook, *Jom*, 2014, **66**(6), p 872–881. https://doi.org/10.1007/s11837-014-0948-5
15. X. Gao, H.Y. Yue, E.J. Guo, S.L. Zhang, L.H. Yao, X.Y. Lin, B. Wang and E.H. Guan, Tribological Properties of Copper Matrix Composites Reinforced with Homogeneously Dispersed graphene Nanosheets, *J. Mater. Sci. Technol.*, 2018, **34**(10), p 1925–1931. https://doi.org/10.1016/j.jmst.2018.02.010
16. W. Xu, R. Hu, J.S. Li and H.Z. Fu, Effect of Electrical Current on Tribological Property of Cu matrix Composite Reinforced by Carbon Nanotubes, *Trans. Nonferrous Metals Soc. China*, 2011, **21**(10), p 2237–2241. https://doi.org/10.1016/S1003-6326(11)61001-7
17. W.X. Chen, J.P. Tu, L.Y. Wang, H.Y. Gan, Z.D. Xu and X.B. Zhang, Tribological Application of Carbon Nanotubes in a Metal-based Composite Coating and Composites, *Carbon*, 2003, **41**(2), p 215–222. https://doi.org/10.1016/S0008-6223(02)00265-8
18. W.Z. Zhai, N. Srikanth, L.B. Kong and K. Zhou, Carbon Nanomaterials in Tribology, *Carbon*, 2017, **119**, p 150–171. https://doi.org/10.1016/j.carbon.2017.04.027
19. M.Y. Zhou, X.N. Qu, L.B. Ren, L.L. Fan, Y.W.X. Zhang, Y.Y. Guo, G.F. Quan, Q. Tang et al., The Effects of Carbon Nanotubes on the Mechanical and Wear Properties of AZ31 Alloy, *Materials*, 2017, **10**(12), p 1–17. https://doi.org/10.3390/ma10121385
20. S.R. Dong, J.P. Tu and X.B. Zhang, An Investigation of the Sliding wear Behavior of Cu-Matrix Composite Reinforced by Carbon Nanotubes, *Mater. Sci. Eng. Struct. Mater. Properties Microstruct. Process.*, 2001, **313**(1–2), p 83–87. https://doi.org/10.1016/S0921-5093(01)00963-7
21. K.T. Kim, S. Cha and S.H. Hong, Hardness and Wear Resistance of Carbon Nanotube Reinforced Cu Matrix Nanocomposites, *Mater. Sci. Eng. Struct. Mater. Properties Microstruct. Process.*, 2007, **449**, p 46–50. https://doi.org/10.1016/j.msea.2006.02.310
22. W. Xu, R. Hu, J.S. Li, Y.Z. Zhang and H.Z. Fu, Tribological Behavior of CNTs-Cu and Graphite-Cu Composites with Electric Current, *Trans. Nonferrous Metals Soc. China*, 2012, **22**(1), p 78–84. https://doi.org/10.1016/S1003-6326(11)61143-6
23. H.Y. Yue, L.H. Yao, X. Gao, S.L. Zhang, E.J. Guo, H. Zhang, X.Y. Lin and B. Wang, Effect of Ball-Milling and Graphene Contents on the Mechanical Properties and Fracture Mechanisms of Graphene Nanosheets Reinforced Copper Matrix Composites, *J. Alloy. Compd.*, 2017, **691**, p 755–762. https://doi.org/10.1016/j.jallcom.2016.08.303
24. Ch. Guiderdoni, E. Pavlenko, V. Turq, A. Weibel, P. Puech, C. Estournès, A. Peigney, W. Bacsa et al., The Preparation of Carbon Nanotube (CNT)/Copper Composites and the Effect of the Number of CNT Walls on Their Hardness, Friction and Wear Properties, *Carbon*, 2013, **58**, p 185–197. https://doi.org/10.1016/j.carbon.2013.02.049
25. Z.X. Huang, Z. Zheng, S. Zhao, S.J. Dong, P. Luo and L. Chen, Copper Matrix Composites Reinforced by Aligned Carbon Nanotubes: Mechanical and Tribological Properties, *Mater. Des.*, 2017, **133**, p 570–578. https://doi.org/10.1016/j.matdes.2016.08.021
26. R. Murugesan, M. Gopal and G. Murali, Effect of Cu, Ni Addition on the CNTs Dispersion, Wear and Thermal Expansion Behavior of Al-CNT Composites by Molecular Mixing and Mechanical Alloying, *Appl. Surf. Sci.*, 2019, **495**, 143542. https://doi.org/10.1016/j.apsusc.2019.143542
27. Z.Y. Hu, Z.H. Zhang, X.W. Cheng, F.C. Wang, Y.F. Zhang and S.L. Li, A Review of Multi-Physicalfields Induced Phenomena and Effects in Spark Plasma Sintering: Fundamentals and Applications, *Mater. Des.*, 2020, **191**, p 1–54. https://doi.org/10.1016/j.matdes.2020.108662
28. H. Wang, Z.H. Zhang, Z.Y. Hu, Q. Song, S.P. Yin and Z. Kang, Improvement of Interfacial Interaction and Mechanical Properties in Copper Matrix Composites Reinforced with Copper Coated Carbon Nanotubes, *Mater. Sci. Eng. Struct. Mater. Properties Microstruct.*

Process., 2018, **715**, p 163–173. https://doi.org/10.1016/j.msea.2018.01.005
29. H. Wang, Z.H. Zhang, H.M. Zhang, Z.Y. Hu, S.L. Li and X.W. Cheng, Novel Synthesizing and Characterization of Copper Matrix Composites Reinforced with Carbon Nanotubes, *Mater. Sci. Eng. Struct. Mater. Properties Microstruct. Process.*, 2017, **696**, p 80–89. https://doi.org/10.1016/j.msea.2017.04.055
30. T. Rodriguez-Suarez, J.F. Bartolome, A. Smirnov, S. Lopez-Esteban, R. Torrecillas and J.S. Moya, Sliding Wear Behaviour of Alumina/Nickel Nanocomposites Processed by a Conventional Sintering Route, *J. Eur. Ceram. Soc.*, 2011, **31**(8), p 1389–1395. https://doi.org/10.1016/j.jeurceramsoc.2011.02.011
31. D. Nayak, N. Ray, R. Sahoo and M. Debata, Analysis of Tribological Performance of Cu Hybrid Composites Reinforced with Graphite and TiC Using Factorial Techniques, *Tribol. Trans.*, 2014, **57**(5), p 908–918. https://doi.org/10.1080/10402004.2014.923079
32. S.M. Javadhesari, S. Alipour and M.R. Akbarpour, Microstructural Characterization and Enhanced Hardness, Wear and Antibacterial Properties of a Powder Metallurgy SiC/Ti-Cu Nanocomposite as a Potential Material for Biomedical Applications, *Ceram. Int.*, 2019, **45**(8), p 10603–10611. https://doi.org/10.1016/j.ceramint.2019.02.127
33. S.L. Fu, X.H. Chen and P. Liu, Preparation of CNTs/Cu Composites with Good Electrical Conductivity and Excellent Mechanical Properties, *Mater. Sci. Eng. Struct. Mater. Prop. Microstruct. Process.*, 2020, **771**, 138656. https://doi.org/10.1016/j.msea.2019.138656
34. H.J. Choi, S.M. Lee and D.H. Bae, Wear Characteristic of Aluminum-Based Composites Containing Multi-Walled Carbon Nanotubes, *Wear*, 2010, **270**(1), p 12–18. https://doi.org/10.1016/j.wear.2010.08.024
35. G.Y. Lee, C.K.H. Dharan and R.O. Ritchie, A Physically-Based Abrasive Wear Model for Composite Materials, *Wear*, 2002, **252**(3–4), p 322–331. https://doi.org/10.1016/S0043-1648(01)00896-1
36. M.A. Shaik and B.R. Golla, Development of Highly Wear Resistant Cu-Al Alloys Processed via Powder Metallurgy, *Tribol. Int.*, 2019, **136**, p 127–139. https://doi.org/10.1016/j.triboint.2019.03.055
37. Y.M. Li, Q.B. Yue, H.Y. Li and H.B. He, Friction and Wear Characteristics of 20Cr Steel Substrate and TiAlN Coating under Different Lubrication Conditions, *Int. J. Precis. Eng. Manuf.*, 2018, **19**(10), p 1521–1528. https://doi.org/10.1007/s12541-018-0179-8
38. P.C. Tsai, Y.R. Jeng, J.T. Lee, I. Stachiv and P. Sittner, Effects of Carbon Nanotube Reinforcement and Grain Size Refinement Mechanical Properties and Wear Behaviors of Carbon Nanotube/Copper Composites, *Diam. Relat. Mater.*, 2017, **74**, p 197–204. https://doi.org/10.1016/j.diamond.2017.03.012
39. N.S. Shaari, J.M. Said, A. Jumahat and M.H. Ismail, Wear Behaviour of Copper/Carbon Nanotubes, *Ind. Lubr. Tribol.*, 2017, **69**(3), p 342–347. https://doi.org/10.1108/ILT-09-2016-0198
40. J.L. Li, L.J. Wang, T. He and W. Jiang, Surface Graphitization and Mechanical Properties of Hot-Pressed Bulk Carbon Nanotubes Compacted by Spark Plasma Sintering, *Carbon*, 2007, **45**(13), p 2636–2642. https://doi.org/10.1016/j.carbon.2007.08.023
41. A.K. Behera, R. Chandran, S. Das and A. Mallik, Wear Performance and Nanomechanical Behavior of Sonoelectroplated Cu-Graphene Nanocomposite Thin Films, *J. Mater. Eng. Perform.*, 2021, **30**(2), p 1398–1410. https://doi.org/10.1007/s11665-020-05355-y
42. V. Testa, S. Morelli, G. Bolelli, L. Lusvarghi, S. Björklund and S. Joshi, Micromechanical Behaviour and Wear Resistance of Hybrid Plasma-Sprayed TiC Reinforced Tribaloy-400, *Surf. Coat. Technol.*, 2021, **425**, p 1–15. https://doi.org/10.1016/j.surfcoat.2021.127682
43. F. Daneshvar, T. Zhang, A. Aziz, H.J. Sue and M.E. Welland, Tuning the Composition and Morphology of Carbon Nanotube-Copper Interface, *Carbon*, 2020, **157**, p 583–593. https://doi.org/10.1016/j.carbon.2019.10.084
44. X.F. Chen, J.M. Tao, J.H. Yi, C.J. Li, R. Bao, Y.C. Liu, X. You and S.L. Tan, Balancing the Strength and Ductility of Carbon Nanotubes Reinforced Copper Matrix Composites with Microlaminated Structure and Interdiffusion Interface, *Mater. Sci. Eng. Struct. Mater. Prop. Microstruct. Process.*, 2018, **712**, p 790–793. https://doi.org/10.1016/j.msea.2017.12.044